beta-Galactosidase enzyme fragment complementation for the measurement of Wnt/beta-catenin signaling

β-Galactosidase enzyme fragment complementation for the measurement of Wnt/β-catenin signaling

Folkert Verkaar,*,† W. Matthijs Blankesteijn,† Jos F. M. Smits,† and Guido J. R. Zaman*,[1]

*Schering-Plough Research Institute, Oss, The Netherlands; and †Department of Pharmacology and Toxicology, Cardiovascular Research Institute Maastricht, Maastricht University, Maastricht, The Netherlands

ABSTRACT **Wnt/β-catenin signaling is an important regulator of cell polarity, proliferation, and stem cell maintenance during development and adulthood. Wnt proteins induce the nuclear accumulation of β-catenin, which regulates the expression of Wnt-responsive genes through association with TCF/LEF transcription factors. Aberrant Wnt/β-catenin signaling has been implicated in a plethora of pathologies and, most notably, underlies initiation and expansion of several cancers. Here, we apply enzyme fragment complementation to measure the nuclear accumulation of β-catenin. β-Catenin was tagged with a peptide fragment of β-galactosidase and transfected into cells expressing a corresponding deletion mutant of the enzyme exclusively in the nucleus. Stimulation of the cells with recombinant Wnt-3a restored β-galactosidase activity in a dose-dependent manner with nanomolar potency. Using the assay, we confirmed that Wnt-5a represses β-catenin-driven reporter gene activity downstream of nuclear entry of β-catenin. In addition, we tested a library of >2000 synthetic chemical compounds for their ability to induce β-catenin nuclear accumulation. The immunosuppressive protein kinase C inhibitor sotrastaurin (AEB-071) was identified as an activator of Wnt/β-catenin signaling at micromolar concentrations. It was confirmed that the compound stabilizes endogenous β-catenin protein and can induce TCF/LEF-dependent gene transcription. Subsequent biochemical profiling of >200 kinases revealed both isoforms of glycogen synthase kinase 3, as previously unappreciated targets of sotrastaurin. We show that the β-catenin nuclear accumulation assay contributes to our knowledge of molecular interactions within the Wnt/β-catenin pathway and can be used to find new therapeutics targeting Wnt/β-catenin signaling.—Verkaar, F., Blankesteijn, W. M., Smits, J. F. M., Zaman, G. J. R. β-Galactosidase enzyme fragment complementation for the measurement of Wnt/β-catenin signaling. *FASEB J.* 24, 1205–1217 (2010). www.fasebj.org**

Key Words: AEB-071 · GSK3 · PKC · sotrastaurin · Wnt-3a · Wnt-5a

WNT/β-CATENIN SIGNALING IS AN evolutionarily conserved signal transduction cascade that plays pivotal roles in embryogenesis and adult stem cell maintenance (1). Signaling through this pathway revolves around the multifunctional protein β-catenin. β-Catenin forms complexes with E-cadherin and α-catenin at the plasma membrane, thereby bridging adhesion proteins to the cytoskeleton. In addition, β-catenin functions as a transcription factor that modulates the expression of Wnt-responsive genes after its translocation from the cytoplasm to the nucleus (2). In quiescent cells, pathway activation is precluded by the phosphorylation of free β-catenin (as opposed to cadherin-bound β-catenin) by a protein assembly termed the "destruction complex." The destruction complex consists of the scaffolding proteins axin and APC, as well as the Ser/Thr kinases glycogen synthase kinase 3 (GSK3) and casein kinase I, which sequentially phosphorylate β-catenin, thereby marking it for proteasomal degradation.

The Wnt/β-catenin pathway is initiated by the binding of Wnt proteins (Wnts) to 7-transmembrane spanning receptors of the Frizzled family and a representative of the low-density lipoprotein receptor-related protein family (LRP5 or LRP6). By a not fully understood mechanism, Frizzled- and LRP5/6-receptor activation interferes with destruction complex function. As a result, unphosphorylated β-catenin accumulates in the cytoplasm and eventually translocates to the nucleus. There, β-catenin forms a coactivator complex with members of the T cell factor/lymphoid enhancer factor (TCF/LEF) family of HMG box DNA-binding proteins to activate Wnt-responsive genes (2).

Nineteen different Wnt genes have been identified in the human genome. In early assays to measure Wnt/β-catenin signaling, not all of these stabilized β-catenin (3, 4). Wnt-5a, for example, antagonizes Wnt/β-catenin signaling *via* the receptor tyrosine kinase-like orphan receptor 2 (ROR2) (5).

Nuclear accumulation of β-catenin has been observed in cancers of the colon, breast, and prostate, and elevated signaling through β-catenin is thought to be an early step in formation of these tumors (6, 7). Abnormal Wnt/β-catenin signaling has also been implicated in several other diseases, including osteoporosis and degenerative disorders (8, 9). Despite its clear links to human pathology, no drugs targeting β-catenin signaling are available. In part, this is due to the lack of robust and accurate assays to

[1] Correspondence: Schering-Plough Research Institute, P.O. Box 20, 5340 BH Oss, The Netherlands. E-mail: guido.zaman@spcorp.com

doi: 10.1096/fj.09-141671

measure Wnt/β-catenin pathway activation in a format suitable for high-throughput screening (HTS). TCF-dependent reporter genes, such as TOPflash, are commonly used to probe Wnt/β-catenin signaling (10, 11). However, reporter gene technologies generally suffer from high false-positive hit rates in HTS (12). Immunocytochemical approaches using specific anti-β-catenin antibodies have been applied (13, 14), but these assays require several washing steps and are therefore unsuitable for automated screening.

Here, we introduce the use of β-galactosidase enzyme fragment complementation (EFC), an assay principle shown to be amenable to HTS (15, 16), to measure nuclear entry of β-catenin. Human β-catenin was genetically fused to a ~4-kDa fragment from *Escherichia coli* β-galactosidase, termed α-peptide (17), and introduced into a cell line expressing a nuclear-targeted complementary β-galactosidase mutant. In the resulting cell line, β-galactosidase activity is dependent on nuclear entry of β-catenin (**Fig. 1**). A similar strategy has been employed previously to measure the nuclear import of the human glucocorticoid receptor (GR) following stimulation with dexamethasone (Dex) (18). After showing that the β-catenin EFC assay accurately reflects β-catenin-dependent signaling, we employed the assay to study the mechanism of Wnt5a-mediated inhibition of Wnt-3a/β-catenin signaling. In addition, we used the assay to screen a library of low molecular weight (LMW) organic synthetic chemicals. This revealed the unanticipated ability of the immunosuppressive drug sotrastaurin (AEB-071) to activate Wnt/β-catenin signaling.

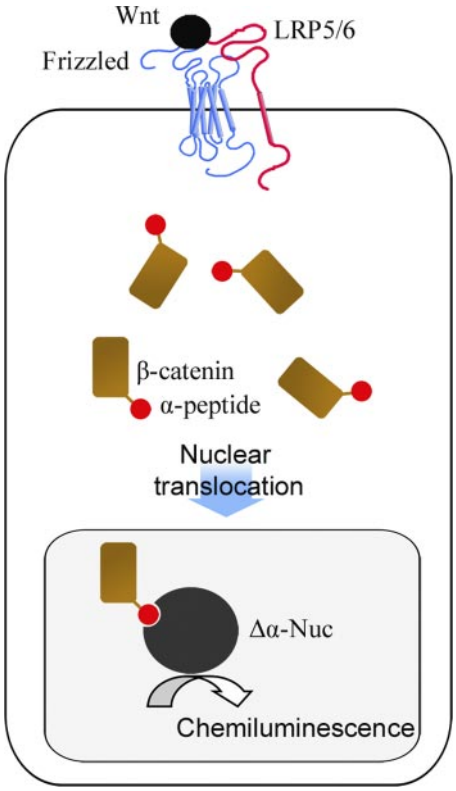

Figure 1. Schematic representation of the principle of the β-catenin EFC assay. α-peptide-tagged β-catenin is stabilized following Wnt treatment, and migrates into the nucleus. There, the α-peptide complements with the Δα-Nuc β-galactosidase mutant. Activity of the reconstituted β-galactosidase enzyme is determined using a chemiluminescent probe.

MATERIALS AND METHODS

Generation of constructs

The β-catenin- and GR-coding sequences were PCR amplified and inserted into pProLabel-C3 (DiscoveRx, Hannover, Germany) using *Kpn*I/*Bam*HI-digestion. SuperTOPflash was kindly provided by Prof. Dr. Randall T. Moon (University of Washington, Seattle, WA, USA). Full-length HA-tagged mouse ROR2 in pcDNA3.1 was a gift from Prof. Dr. Yasuhiro Minami (Kobe University, Kobe, Japan). HA-tagged Wnt-coding cDNAs in pLNC were kindly provided by Dr. Jan Kitajewski (Columbia University, New York, NY, USA). pRL-Null was purchased from Promega (Leiden, The Netherlands).

Chemicals and reagents

Actinomycin D, cycloheximide, LiCl, MG132, and dexamethasone were purchased from Sigma-Aldrich (Steinheim, Germany). The 5-nitropyridine PKC inhibitor 1 is compound 19 exemplified in ref. 36. The 4-aryl pyrimidine PKC inhibitor 2 is compound 1 exemplified in ref. 37. All LMW compounds were synthesized at Schering-Plough. Recombinant mouse Wnt-3a and Wnt-5a were obtained from R&D Systems (Abingdon, UK).

Cell culture and stable transfections

Jurkat, U2OS, and HEK293T cells (obtained from the American Type Culture Collection, Manassas, VA, USA) were subcultured biweekly in DMEM F12 (Invitrogen, Leek, The Netherlands) supplemented with 10% FCS (Cambrex, Verviers, Belgium), 100 U/ml penicillin, and 100 μg/ml streptomycin (Invitrogen). To this medium, 500 μg/ml neomycin (Sigma-Aldrich) was added to culture U2OS-β-catenin-GFP cells. U2OS-Δα-Nuc and HEK293-Δα-Nuc cells (both from DiscoveRx) were grown in medium supplemented with 150 μg/ml hygromycin (Invitrogen). Stable transfection of α-peptide-tagged β-catenin- and GR-constructs was performed using Fugene 6 reagent (Roche Applied Science, Indianapolis, IN, USA), according to the manufacturer's instructions. Forty-eight hours after transfection, cells were harvested in growth medium containing 150 μg/ml hygromycin and 500 μg/ml neomycin (Sigma-Aldrich) and seeded in 96-well plates for single-cell clone selection by means of limited dilution.

Western and Eastern blot analysis

Cytosolic fractions were prepared as described by Mikels and Nusse (5). Total cell lysates were prepared in lysis buffer [150 mM NaCl, 5 mM EDTA, 50 mM Tris, 0.1% (v/v) SDS, and 1% (v/v) Nonidet P-40 (Roche Applied Science), pH 7.5] containing Complete protease inhibitor cocktail (Roche Applied Science). For cellular fractionation experiments, cells were incubated in hypotonic lysis buffer (10 mM HEPES, 1.5 mM $MgCl_2$, 10 mM KCl, and 0.5 mM DTT, pH 7.9) and lysed by addition of Nonidet P-40 to a final concentration of 1% (v/v). Nuclei were pelleted at 16,000 *g* for 5 min, and supernatant containing cytoplasmic proteins was removed promptly. Nuclei were resuspended in 20 mM HEPES, 1.5 mM $MgCl_2$, 420 mM NaCl, 0.2 mM EDTA, and 25% glycerol (v/v), at pH 7.9. Nuclear debris was pelleted (16,000 *g* for 5 min), and supernatant with nuclear proteins was collected.

Lysates were separated by SDS-PAGE using 4–12% Bis/Tris polyacrylamide gels (Invitrogen) followed by transfer to nitrocellulose using the iBlot blotting system (Invitrogen). Subsequently, Eastern blotting was performed according to the manufacturer's instructions (DiscoveRx). For Western blot analysis, blots were blocked in 1× washing buffer (BioMérieux, Boxtel, The Netherlands) containing 5% skim milk (Difco, Leeuwarden, The Netherlands) for 1 h at room temperature. Primary antibodies were incubated with the blot overnight at 4°C in washing buffer supplemented with 1% skim milk at the indicated dilutions: rat anti-HA-HRP, 1:1000 (clone 3F10; Roche Applied Science); mouse anti-β-catenin, 1:2000 (BD Transduction Laboratories, Lexington, KY, USA); mouse anti-β-actin, 1:5000, and mouse anti-α-tubulin, 1:10,000 (Abcam, Cambridge, UK); mouse anti-EA, 1:5000 (DiscoveRx); rabbit anti-TCF-4, 1:1000; rabbit anti-LRP6, 1:1000; and rabbit anti-phospho-LRP6, 1:1000 (Cell Signaling Technology; Danvers, MA, USA). The blots were washed with washing buffer and incubated with anti-mouse-HRP conjugate (1:2000; Promega) or anti-rabbit-HRP conjugate (1:1000; Promega) for 1 h at room temperature, and immunocomplexes were visualized with chemiluminescence detection using SuperSignal West Dura Extended Duration Substrate (Perbio, Aalst, Belgium).

Enzyme fragment complementation assays

Cells were seeded in a 384-well CulturPlate (Perkin Elmer, Boston, MA, USA) with 0.5×10^4 U2OS-EFC cells or 2×10^4 HEK293-EFC cells in 25 μl DMEM F12 containing 2% FCS, 100 U/ml penicillin and 100 μg/ml streptomycin (assay medium). After overnight incubation at 37°C in a humidified incubator (5% CO_2, 95% humidity), cells were stimulated with 2.5 μl agonist in assay medium and then returned to the incubator for 3 h. Cells were disrupted using 12.5 μl substrate-containing lysis buffer from the PathHunter Detection Kit in the formulation specified by the supplier (DiscoveRx). Plates were incubated in the dark for 1 h at room temperature before measurement of β-galactosidase activity (luminescence) on an Envision multilabel plate reader (PerkinElmer).

siRNA transfection

Nontargeting siRNA controls and siRNA targeting β-catenin (Thermo Fisher/Dharmacon, Lafayette, CO, USA) were transfected into cells using Lipofectamine 2000 (Invitrogen) according to the manufacturer's instructions, at a final concentration of 100 nM. Cells were cultured further for 72 h before EFC assays were performed or before harvesting for total cell lysate preparation as described above.

Luciferase assays

Cells were transiently transfected with Fugene 6 reagent (Roche Applied Science) in a 6-well plate, according to the manufacturer's protocol. Each well received 2 μg DNA, *i.e.*, 100 ng pRL-Null (Promega), 1400 ng SuperTOPflash (25) and 500 ng pcDNA3.1-ROR2-HA, pProLabel-β-catenin S37A, or corresponding empty vector. Twenty-four hours post-transfection, 2×10^4 cells (U2OS) or 5×10^4 cells (HEK293T) were transferred to 96-well CulturPlates (PerkinElmer) coated with poly-L-lysine (Sigma-Aldrich) and were cultured overnight. Growth medium was replaced by assay medium (DMEM F12 containing 2% FCS, 100 U/ml penicillin and 100 μg/ml streptomycin) containing agonists at the concentrations indicated in the text, and cells were incubated overnight at 37°C. Luciferase activities were measured on an Envision multilabel plate reader by use of the Dual Luciferase Reporter assay system (Promega).

Fluorescence microscopy

U2OS-β-catenin-GFP cells were plated at 2×10^4 cells/100 μl DMEM F12 supplemented with 10% FCS in a 96-well black-view plate (PerkinElmer) and allowed to adhere overnight. The following day, medium was aspired and replaced with DMEM F12 containing 10% FCS and agonists as indicated. Cells were fixed in 4% (v/v) paraformaldehyde (BioConnect, Huissen, The Netherlands) the next day and incubated with 1 μM Hoechst (Invitrogen) in PBS until plates were analyzed on a Discovery One automated inverted fluorescence microscope (Molecular Devices, Sunnyvale, CA, USA)

Data representation

EC_{50} values for rmWnt-3a and rmWnt-5a dose response curves were calculated from the expected molecular mass of recombinant mouse Wnt-3a (41 kDa) and recombinant mouse Wnt-5a (45 kDa) using GraphPad Prism 4.0 software (GraphPad, San Diego, CA, USA). All data are represented as averages ± SE. Statistical significance of observed differences was determined using Student's *t* test and is indicated in the figures. Values of $P < 0.05$ were regarded as statistically significant.

RESULTS

Development of β-catenin enzyme fragment complementation assay

Human β-catenin was C-terminally tagged with a peptide corresponding to aa 3–92 of *E. coli* β-galactosidase (termed α-peptide) (17). The chimeric protein was introduced into a U2OS human osteosarcoma cell line stably overexpressing a nuclear-localized complementary deletion mutant of β-galactosidase (U2OS-Δα-Nuc). The resultant cell line was named U2OS-EFC. The expression of the Δα-Nuc protein in U2OS-Δα-Nuc and U2OS-EFC cells was verified by Western blot analysis (**Fig. 2*A***). In addition, cell fractionation experiments confirmed that Δα-Nuc was expressed in the nucleus and not in the cytoplasm of U2OS-EFC cells (Fig. 2*B*). The expression of β-catenin in cell lysates from U2OS, U2OS-Δα-Nuc, and U2OS-EFC cells was also examined (Fig. 2*C*). Two bands were detected with anti-β-catenin antibody in U2OS-EFC cells, consistent with the expression of both α-peptide-tagged and nonmodified β-catenin in these cells (Fig. 2*C*). Only one high-mobility band was found in U2OS and U2OS-Δα-Nuc cells (Fig. 2*C*). To verify that the additional band detected in cell lysates from U2OS-EFC corresponds to α-peptide-tagged protein, Eastern blot analysis was performed. In Eastern blotting, protein blots are saturated with purified Δα protein, followed by chemiluminescent detection of complemented β-galactosidase (19). As expected, a single protein band corresponding to α-peptide-tagged β-catenin was observed, whereas no bands were detected in lysates from U2OS and U2OS-Δα-Nuc cells (Fig. 2*D*). We then assessed whether activation of the Wnt/β-catenin pathway could increase β-galactosidase activity in the U2OS-EFC cell line. Cells were stimulated with 25 nM (1000 ng/ml) recombinant mouse Wnt-3a (rmWnt-3a), which induces β-catenin-dependent signaling through binding to Frizzled receptors (3, 20, 21). Furthermore, the cells were treated

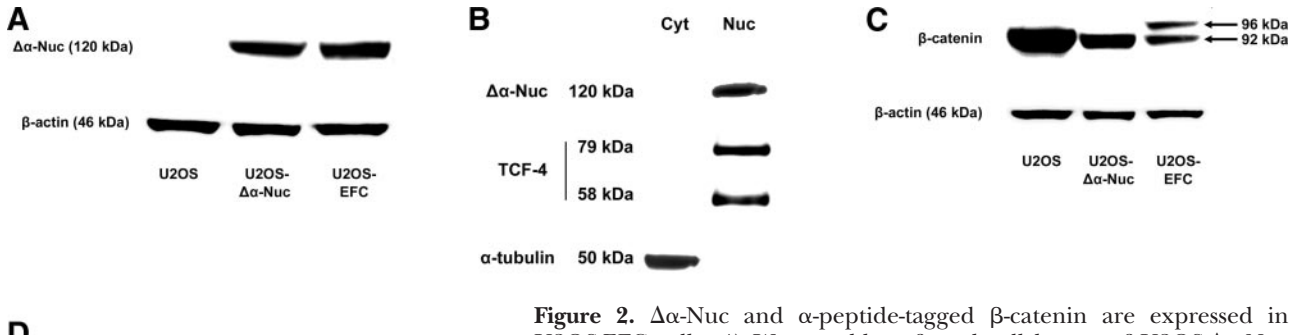

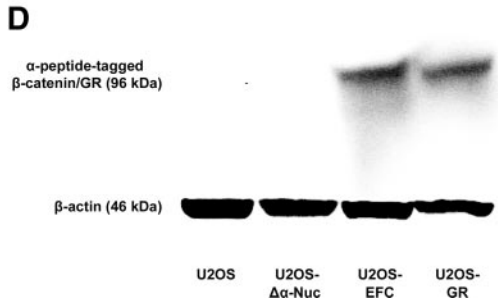

Figure 2. Δα-Nuc and α-peptide-tagged β-catenin are expressed in U2OS-EFC cells. *A*) Western blot of total cell lysates of U2OS-Δα-Nuc and U2OS-EFC cells probed with antibodies against Δα-Nuc. Nontransfected U2OS cells from the American Type Culture Collection were included as a control in the first lane. *B*) Western blot of cytoplasmic (Cyt) and nuclear (Nuc) fractions obtained by hypotonic lysis of U2OS-EFC cells probed with antibodies against Δα-Nuc. TCF-4 and α-tubulin were used as markers of nuclear and cytoplasmic localization, respectively. *C*) Western blot analysis of β-catenin expression in U2OS, U2OS-Δα-Nuc, and U2OS-EFC cells. U2OS cell line is from a different source (American Type Culture Collection) and shows higher expression of endogenous β-catenin than the U2OS-Δα-Nuc cell line (from DiscoveRx) and the derived U2OS-EFC (generated at Schering-Plough). *D*) Eastern blotting of total cell lysates from U2OS, U2OS-Δα-Nuc, and U2OS-EFC to detect α-peptide-tagged protein. Cellular extract from α-peptide-tagged GR-expressing (U2OS-GR) cells was blotted as a positive control. β-Actin was immunostained as a loading control.

with 30 mM lithium chloride (LiCl), which prohibits β-catenin degradation by inhibiting GSK3 (22), or 20 μM MG132, which prevents degradation of β-catenin by the proteasome (23). As a positive reference, the U2OS-Δα-Nuc cells were transiently transfected with a construct encoding α-peptide-tagged β-catenin S37A, a β-catenin mutant that lacks a pivotal phosphorylation site for GSK3, rendering it refractory to proteasomal degradation (24). As shown in **Fig. 3*A***, β-galactosidase activity is only increased in U2OS-Δα-Nuc cells transfected with the α-peptide-tagged β-catenin S37A construct. In contrast, U2OS-EFC cells responded with a marked increase in β-galactosidase activity, when treated with rmWnt-3a, LiCl, or MG132 (Fig. 3*B*). The increase in assay signal correlated well with β-catenin stabilization, as assessed by Western and Eastern blot analysis (Fig. 3*C*). We also measured Wnt/β-catenin signaling using a SuperTOPflash luciferase reporter gene (25). As indicated in Fig. 3*D*, β-catenin-dependent transcriptional activation as determined with SuperTOPflash, correlated well with β-catenin nuclear accumulation as measured with the EFC assay (Fig. 3*B*). We also tested whether we could measure β-galactosidase complementation when U2OS-EFC cells were transiently transfected with plasmids encoding several HA-tagged Wnt proteins (Fig. 3*E*). Results from the EFC assay (Fig. 3*F*) were in agreement with SuperTOPflash activity measured in the same cells (Fig. 3*G*). As a control, cells were transfected with a reporter gene carrying mutations that abolish TCF-binding (FOPflash). Luciferase activity was not induced in cells transfected with this construct (Fig. 3*G*).

We further characterized the pharmacology of the U2OS-EFC cell line using rmWnt-3a to induce β-catenin nuclear accumulation. **Figure 4*A*** shows a representative dose-response curve of U2OS-EFC cells stimulated with increasing concentrations of rmWnt-3a. The half-maximal effective concentration (EC_{50}) was 2.6 ± 1.1 nM (average±SD, n=21), which is in agreement with the EC_{50} of Wnt-3a on SuperTOPflash readout (Fig. 4*B*).

Next, we monitored the assay signal in U2OS-EFC cells that had been stimulated with 25 nM rmWnt-3a in time. β-Galactosidase activity was apparent 30–40 min after addition of Wnt-3a and steadily increased until a plateau was reached after ~150 min (**Fig. 5*A***). These kinetics are consistent with the stabilization of endogenous β-catenin following Wnt treatment, as reported by others (26, 27). For comparison, we followed the development of β-galactosidase activity in time in U2OS-GR cells on treatment with Dex. Treatment with 1 μM Dex induced β-galactosidase complementation within 20 min ($t_{1/2}$~45 min), reaching maximum stimulation after ~90 min (Fig. 5*B*).

Wnt-stimulated β-catenin accumulation has been shown to be dependent on new protein synthesis due to a relief of translational repression, but does not involve gene transcription in several systems (26, 28). To investigate the role of β-catenin gene transcription and translation in the EFC assay, experiments were carried out with the transcription blocker actinomycin D (actD) and the translation inhibitor cycloheximide (CHX). An EFC assay measuring nuclear accumulation of GR on stimulation with Dex was used as a control. Treatment with 1 μM actD caused a slight decrease in assay window in the β-catenin assay (**Fig. 6*A***). However, this effect was probably not specific, as it was also observed for actD-treated U2OS-GR cells following Dex treatment (Fig. 6*B*). In contrast, treatment of U2OS-EFC cells with 100 ng/ml CHX completely inhibited Wnt-3a-stimulated β-galactosidase complementation (Fig. 6*A*). CHX only marginally affected β-galactosidase activity in U2OS-GR cells (Fig. 6*B*). These data demonstrate that β-galactosidase activity in the U2OS-EFC cell line is dependent on translation and not transcription. Nuclear entry of GR was dependent on neither translation nor transcription. These observations are consistent with the

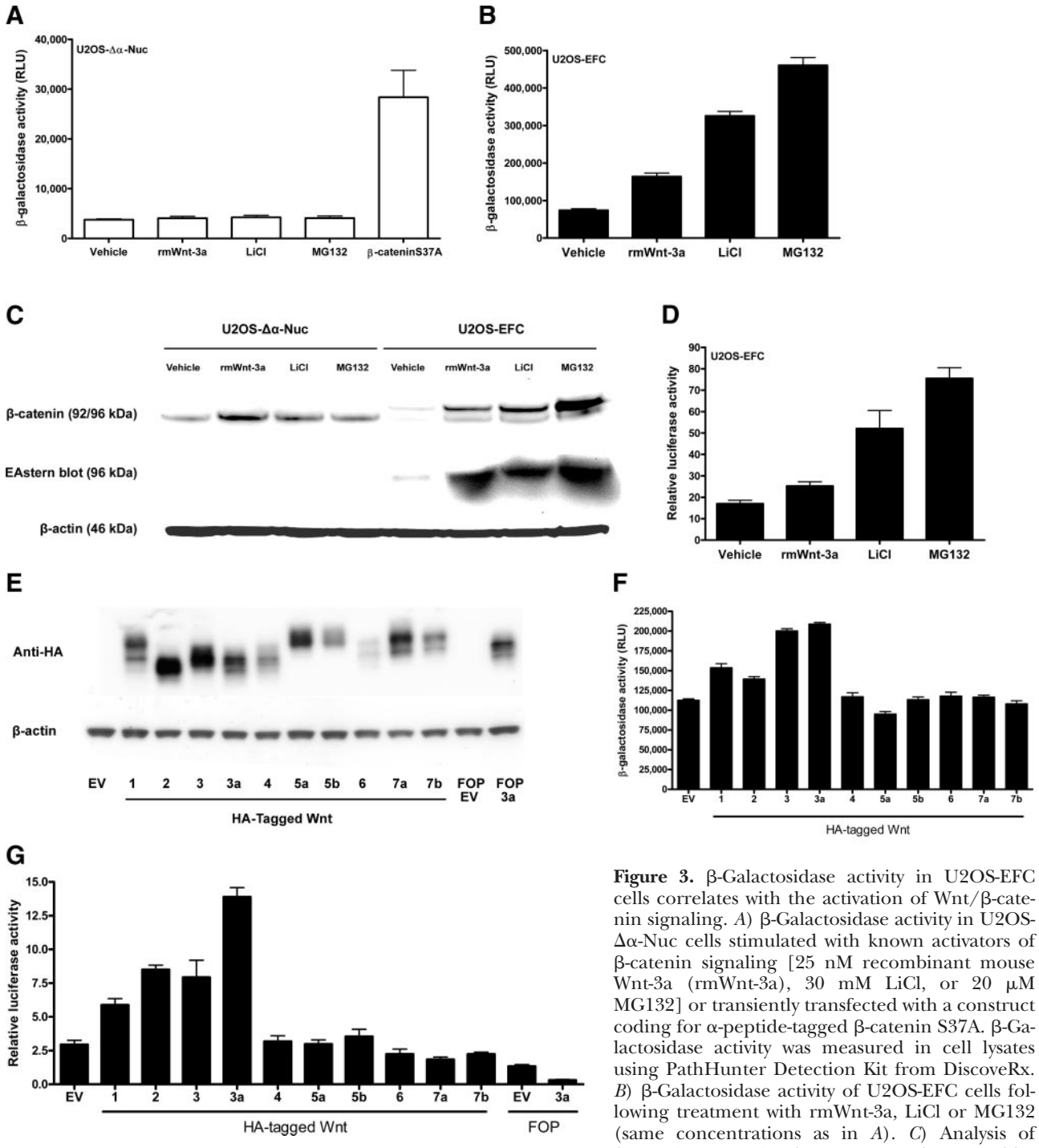

Figure 3. β-Galactosidase activity in U2OS-EFC cells correlates with the activation of Wnt/β-catenin signaling. *A*) β-Galactosidase activity in U2OS-Δα-Nuc cells stimulated with known activators of β-catenin signaling [25 nM recombinant mouse Wnt-3a (rmWnt-3a), 30 mM LiCl, or 20 μM MG132] or transiently transfected with a construct coding for α-peptide-tagged β-catenin S37A. β-Galactosidase activity was measured in cell lysates using PathHunter Detection Kit from DiscoveRx. *B*) β-Galactosidase activity of U2OS-EFC cells following treatment with rmWnt-3a, LiCl or MG132 (same concentrations as in *A*). *C*) Analysis of β-catenin expression by Western and Eastern blot analysis of cytoplasmic fractions from U2OS-Δα-Nuc and U2OS-EFC cells, following stimulation with rmWnt-3a, LiCl, or MG132. *D*) Relative luciferase activity in U2OS-EFC cells transiently transfected with SuperTOPflash reporter plasmid and stimulated with rmWnt-3a, LiCl, or MG132. *E*) Western blot of total cell lysates of U2OS-EFC cells transiently transfected with coding vectors for HA-tagged mouse Wnt-1, -2, -3, -3a, -4, -5a, -5b, -6, -7a, and -7b or empty vector (EV), probed with anti-HA- and anti-β-actin antibodies. *F*) β-Galactosidase activity of U2OS-EFC cells transiently transfected with HA-tagged Wnt-coding vectors or EV. *G*) Luciferase reporter gene activity of U2OS-EFC cells transiently transfected with mouse Wnt coding vectors or EV and SuperTOPflash or FOPflash (FOP) reporter gene construct.

delayed onset and lower rate of nuclear accumulation of β-catenin in comparison to GR (Fig. 5).

To further substantiate that β-galactosidase activity in U2OS-EFC cells is β-catenin dependent, we transfected these cells with siRNAs targeting β-catenin. Western blot analysis of cell lysates of siRNA-treated cells confirmed efficient knockdown of β-catenin, which was not seen with two control siRNAs (**Fig. 7*A***). When tested for β-galactosidase activity, cells transfected with β-catenin siRNA exhibited substantially lower basal β-galactosidase activity (Fig. 7*B*). In addition, their ability to respond to rmWnt-3a (Fig. 7*B*), LiCl, and MG132 was

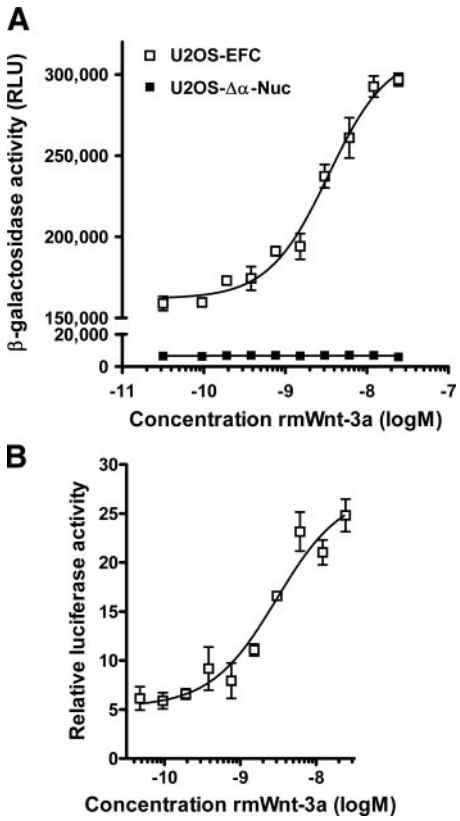

Figure 4. Dose-dependent increase of β-galactosidase activity in U2OS-EFC cells stimulated with rmWnt-3a. *A*) β-Galactosidase activity in U2OS-EFC and U2OS-Δα-Nuc cells stimulated for 3 h with increasing concentrations of rmWnt-3a. *B*) SuperTOPflash reporter gene activity in U2OS-EFC cells treated with increasing doses of rmWnt-3a.

severely blunted (Fig. 7*C*). To verify that the decrease in assay window was not caused by an inability of the cells to respond to Wnt stimulation, LRP6 phosphorylation was examined by Western blot analysis. Phosphorylation of the intracellular tail of LRP6 is an early step in Wnt/β-catenin signaling (29). As can be seen in Fig. 7*D*, Wnt-3a-stimulated LRP6 phosphorylation was not affected by β-catenin siRNA.

Measurement of β-catenin nuclear translocation in Wnt-5a-treated cells

To exemplify the applicability of β-catenin EFC as a basic research tool, we studied β-catenin nuclear accumulation in Wnt-5a-treated cells. Inhibition of Wnt/β-catenin signaling by Wnt-5a has been observed in a variety of assay systems (30, 31). However, current reports are in disagreement on whether β-catenin stability and nuclear translocation are altered by Wnt-5a-treatment. Topol *et al.* (31) have reported the GSK3-independent proteasomal degradation of β-catenin (31). In contrast, data from Mikels and Nusse (5) suggest that Wnt-5a interferes with Wnt/β-catenin signal transduction downstream of β-catenin nuclear entry (5). To address this controversy, U2OS-EFC cells were transiently transfected with SuperTOPflash reporter gene and a vector encoding HA-tagged ROR2, a receptor for Wnt-5a (5). Western blot analysis confirmed expression of HA-tagged ROR2 (Supplemental Fig. S1). Stimulation of cells with 5 nM (200 ng/ml) rmWnt-3a increased SuperTOPflash activity (**Fig. 8*A***). In contrast, incubation with 18 nM (800 ng/ml) recombinant mouse Wnt-5a (rmWnt-5a) did not increase reporter gene activity (Fig. 8*A*). However, Wnt-5a could dose dependently inhibit Wnt-3a-induced SuperTOPflash activity in cells transfected with ROR2 expression vector (Fig. 8*B*). In accordance with the SuperTOPflash reporter gene assay data, mRNA levels of the Wnt-responsive gene axin2 in ROR2-transfected U2OS-EFC cells were increased by 5 nM rmWnt-3a treatment, and reduced to vehicle levels by costimulation with 18 nM rmWnt-5a (Supplemental Fig. S2). The effect was not observed in cells lacking ROR2 overexpression (Fig. 8*B*), despite the fact that endogenously expressed ROR2 could be detected in the U2OS-EFC cell line by qPCR. Likewise, in empty vector-transfected U2OS-EFC cells, the dose-dependent activation of SuperTOPflash in response to rmWnt-3a was unimpaired by coincubation with 18 nM rmWnt-5a (Supplemental Fig. S3).

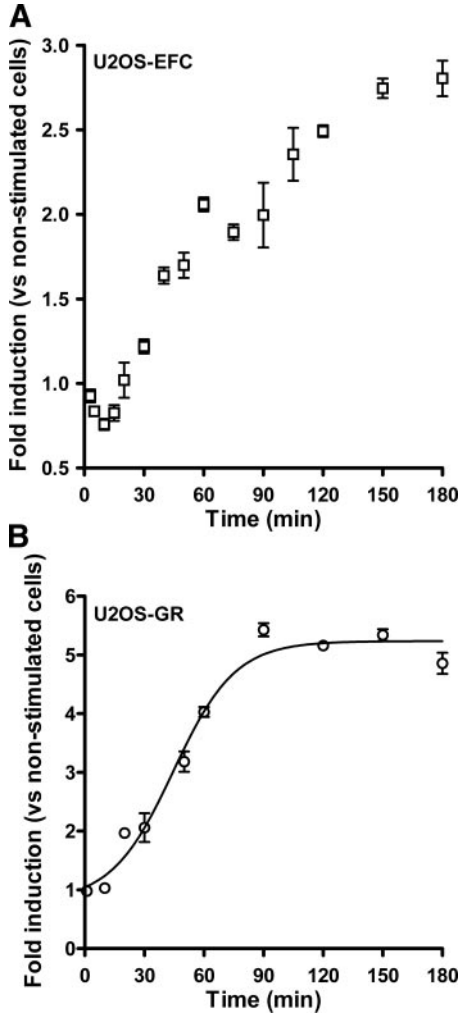

Figure 5. Kinetics of Wnt-stimulated nuclear entry of β-catenin. *A*) β-Galactosidase activity of U2OS-EFC cells stimulated with 25 nM rmWnt-3a from 1 min up to 3 h. *B*) β-Galactosidase activity of U2OS-GR cells stimulated with 1 μM of dexamethasone from 1 min up to 3 h.

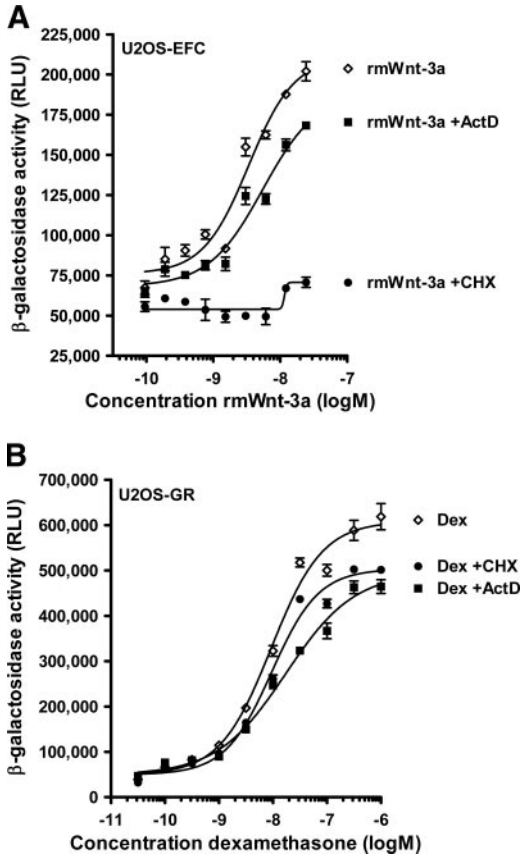

Figure 6. rmWnt-3a-stimulated β-galactosidase activation in U2OS-EFC cells is translation dependent and transcription independent. *A*) β-Galactosidase activity in U2OS-EFC cells stimulated with increasing doses of rmWnt-3a in the absence and presence of treatment with 1 μM actinomycin D (ActD) or 100 μg/ml cycloheximide (CHX). *B*) β-Galactosidase activity in U2OS-GR cells stimulated with increasing concentrations of dexamethasone cotreated with 1 μM ActD or 100 μg/ml CHX.

When normalized for background SuperTOPflash activity, empty vector-transfected U2OS-EFC cells treated with rmWnt-5a or vehicle responded to rmWnt-3a with comparable amplitude and potency (Fig. 8*C*). Because U2OS-EFC cells were unresponsive to rmWnt-5a in terms of β-catenin signaling, unless transfected with ROR2, we considered them as a suitable negative control for Wnt-5a/ROR2-mediated inhibition in further experiments. ROR2 transfection did not alter the potency of rmWnt-3a with regard to SuperTOPflash activation, although a slight decrease in both basal and maximum reporter gene activity was observed (Fig. 8*D*). Treatment of ROR2-transfected U2OS-EFC cells with increasing doses of rmWnt-5a in the presence of 5 nM rmWnt-3a caused a dose-dependent repression of SuperTOPflash reporter gene activity (Fig. 8*B*). Reciprocally, Wnt-3a-induced β-catenin-dependent gene transcription was strongly inhibited in ROR2-transfected U2OS-EFC cells costimulated with 18 nM rmWnt-5a (Fig. 8*E*). When ROR2-overexpressing cells were tested for nuclear accumulation of β-catenin with the EFC assay, we found that rmWnt-3a induced nuclear accumulation of β-catenin in empty vector-transfected and ROR2-transfected U2OS-EFC cells with similar potencies (**Fig. 9*A***). In contrast, rmWnt-5a did not activate β-catenin translocation in empty vector-transfected (Fig. 9*B*), or ROR2-transfected cells (Fig. 9*C*). Increasing doses of rmWnt-5a also did not repress the β-galactosidase complementation in empty vector-transfected and ROR2-transfected U2OS-EFC cells elicited by 5 nM rmWnt-3a (Fig. 9*D*). Even in the presence of rmWnt-5a at a concentration that abrogates β-catenin-driven transcription (*i.e.*, 18 nM; Fig. 8*E*), rmWnt-3a still induced a dose-dependent increase in β-catenin nuclear translocation in ROR2-transfected U2OS-EFC cells that was similar in potency and magnitude to that observed for empty vector-transfected cells (Fig. 9*E*). To examine whether Wnt-5a/ROR2 signaling affects β-catenin stability, Western blot analysis was performed on cytoplasmic fractions from U2OS-EFC cells transfected with either ROR2-coding vector, or corresponding empty vector, and stimulated with rmWnt-3a, rmWnt-5a, or a combination of both ligands. As shown in Fig. 9*F*, rmWnt-3a induced cytoplasmic β-catenin levels were comparable in the absence and presence of rmWnt-5a at a concentration (18 nM) that ablated β-catenin-driven reporter gene activity in ROR2-transfected cells (Fig. 8*E*).

To verify that the unaffected nuclear translocation of β-catenin in rmWnt-5a-treated cells was not a specific property of U2OS cells, we extended our analysis of the site of interaction of rmWnt-3a/β-catenin and rmWnt-5a/ROR2 signaling to another cell line. We stably transfected Δα-Nuc and α-peptide-tagged β-catenin into HEK293 cells to enable measurement of β-catenin nuclear translocation in this cellular background (HEK293-EFC cells). Like the U2OS-EFC cells, HEK293-EFC cells increased β-galactosidase activity in response to rmWnt-3a in a dose-dependent manner, but not in response to Wnt-5a (**Fig. 10*A***). On transfection of SuperTOPflash reporter gene construct and either ROR2-coding vector or corresponding empty vector, HEK293-EFC cells responded to rmWnt-3a treatment with a robust activation of the SuperTOPflash reporter gene (Fig. 10*B*). In contrast to U2OS-EFC cells, rmWnt-5a-mediated inhibition of β-catenin-dependent signaling was readily observed in empty vector-transfected HEK293-EFC cells, while rmWnt-5a-controlled transcriptional repression of SuperTOPflash was further increased in ROR2-transfected cells (Fig. 10*B*). Like for the U2OS-EFC cells (Fig. 9*D*), both empty vector- and ROR2-transfected HEK293-EFC cells did not display any decrease in rmWnt-3a-induced β-catenin translocation in response to increasing concentrations of rmWnt-5a (Fig. 10*C*). Furthermore, rmWnt-3a could still dose dependently increase nuclear β-catenin levels in ROR2-transfected HEK293-EFC cells in the presence of 18 nM rmWnt-5a (Supplemental Fig. S4). When corrected for background β-galactosidase activity, the dose-dependent increase of β-galactosidase complementation in ROR2-transfected HEK293 cells following rmWnt-3a treatment was comparable in the presence or absence of 18 nM rmWnt-5a (Fig. 10*D*).

We conclude that rmWnt-5a does not influence β-catenin stability or nuclear entry and argue for a role for Wnt-5a/ROR2 in transcriptional control of β-catenin target genes.

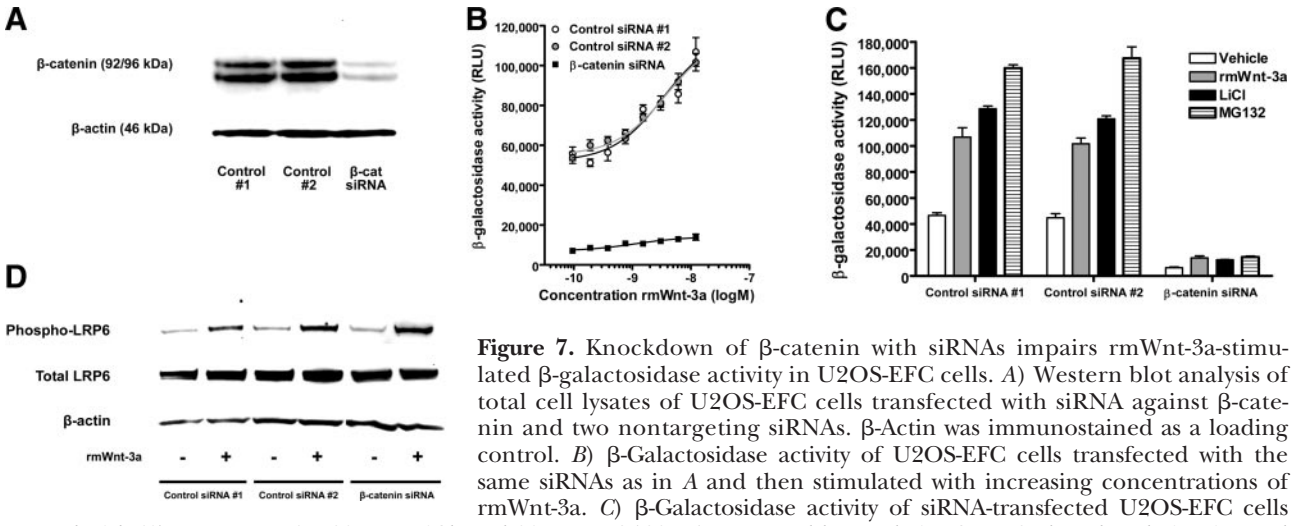

Figure 7. Knockdown of β-catenin with siRNAs impairs rmWnt-3a-stimulated β-galactosidase activity in U2OS-EFC cells. *A*) Western blot analysis of total cell lysates of U2OS-EFC cells transfected with siRNA against β-catenin and two nontargeting siRNAs. β-Actin was immunostained as a loading control. *B*) β-Galactosidase activity of U2OS-EFC cells transfected with the same siRNAs as in *A* and then stimulated with increasing concentrations of rmWnt-3a. *C*) β-Galactosidase activity of siRNA-transfected U2OS-EFC cells treated with 25 nM rmWnt-3a, 30 mM LiCl, and 20 μM MG132. *D*) Western blot analysis of LRP6 phosphorylation in total cell lysates of siRNA-transfected U2OS-EFC cells stimulated with 25 nM rmWnt-3a or vehicle. The blot was stained with anti-phospho-LRP6 antibodies or antibodies detecting total LRP6.

Identification of sotrastaurin as an activator of β-catenin nuclear accumulation

The β-catenin EFC assay was optimized for automated screening and validated for HTS by screening a library of 2318 LMW molecules. The library was enriched for compounds acting on 7-transmembrane receptors or protein kinases, as the aim of the project was to identify new probes for Frizzled receptors and downstream signaling mediators. With an average signal-to-background for rmWnt-3a of 4.3 and a *Z′* factor (32) of 0.51, the assay displayed robust statistics. Three compounds activating β-catenin EFC significantly above background at 10 μM were identified. The activity of these three compounds was confirmed in separate assays and on retesting from a different stock solution. One of the compounds was identified as sotrastaurin (AEB-071) (**Fig. 11*A***), an investigational immunosuppressive pan-protein kinase C (PKC)-inhibiting drug developed by Novartis Pharmaceu-

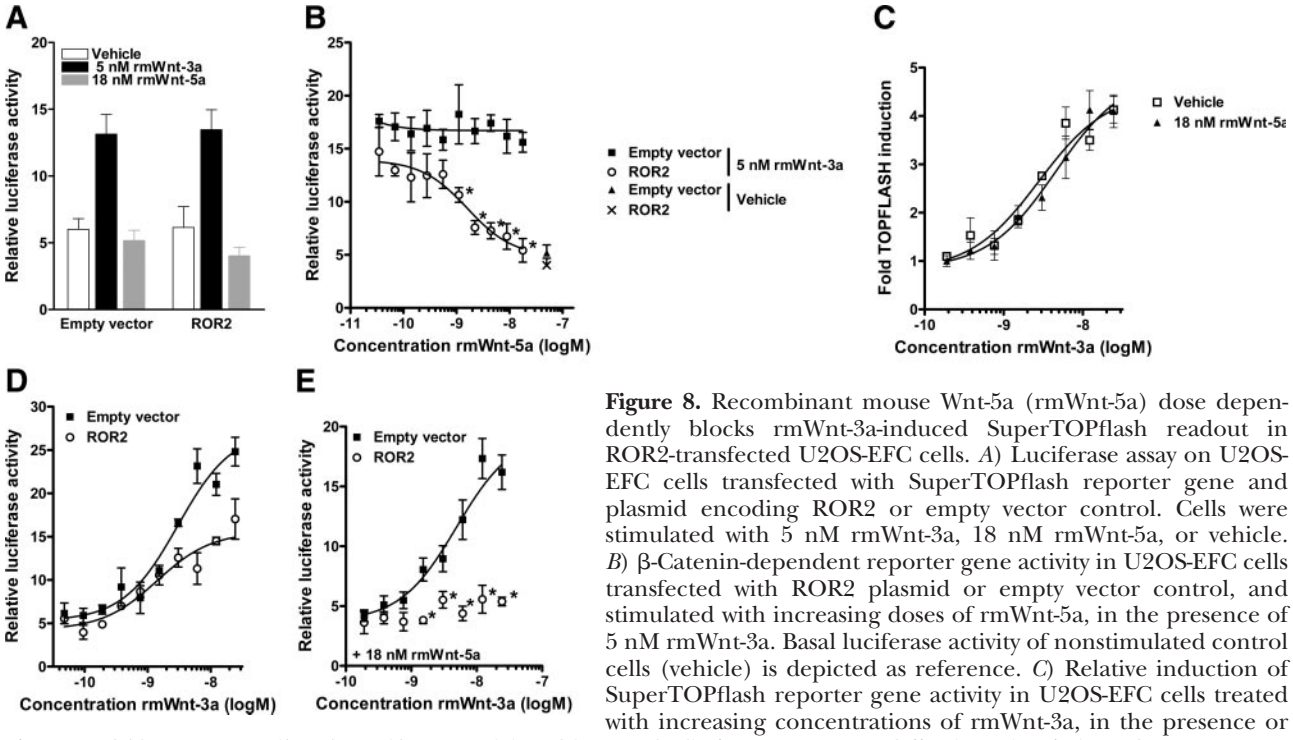

Figure 8. Recombinant mouse Wnt-5a (rmWnt-5a) dose dependently blocks rmWnt-3a-induced SuperTOPflash readout in ROR2-transfected U2OS-EFC cells. *A*) Luciferase assay on U2OS-EFC cells transfected with SuperTOPflash reporter gene and plasmid encoding ROR2 or empty vector control. Cells were stimulated with 5 nM rmWnt-3a, 18 nM rmWnt-5a, or vehicle. *B*) β-Catenin-dependent reporter gene activity in U2OS-EFC cells transfected with ROR2 plasmid or empty vector control, and stimulated with increasing doses of rmWnt-5a, in the presence of 5 nM rmWnt-3a. Basal luciferase activity of nonstimulated control cells (vehicle) is depicted as reference. *C*) Relative induction of SuperTOPflash reporter gene activity in U2OS-EFC cells treated with increasing concentrations of rmWnt-3a, in the presence or absence of 18 nM rmWnt-5a. *D*) Luciferase activity of SuperTOPflash reporter gene following stimulation of empty vector- and ROR2-transfected U2OS-EFC cells with increasing concentrations of rmWnt-3a. *E*) SuperTOPflash reporter gene activity of empty vector- and ROR2-transfected U2OS-EFC cells stimulated with increasing concentrations of rmWnt-3a when costimulated with 18 nM rmWnt-5a. $*P < 0.05$ *vs.* empty vector control; Student's *t* test.

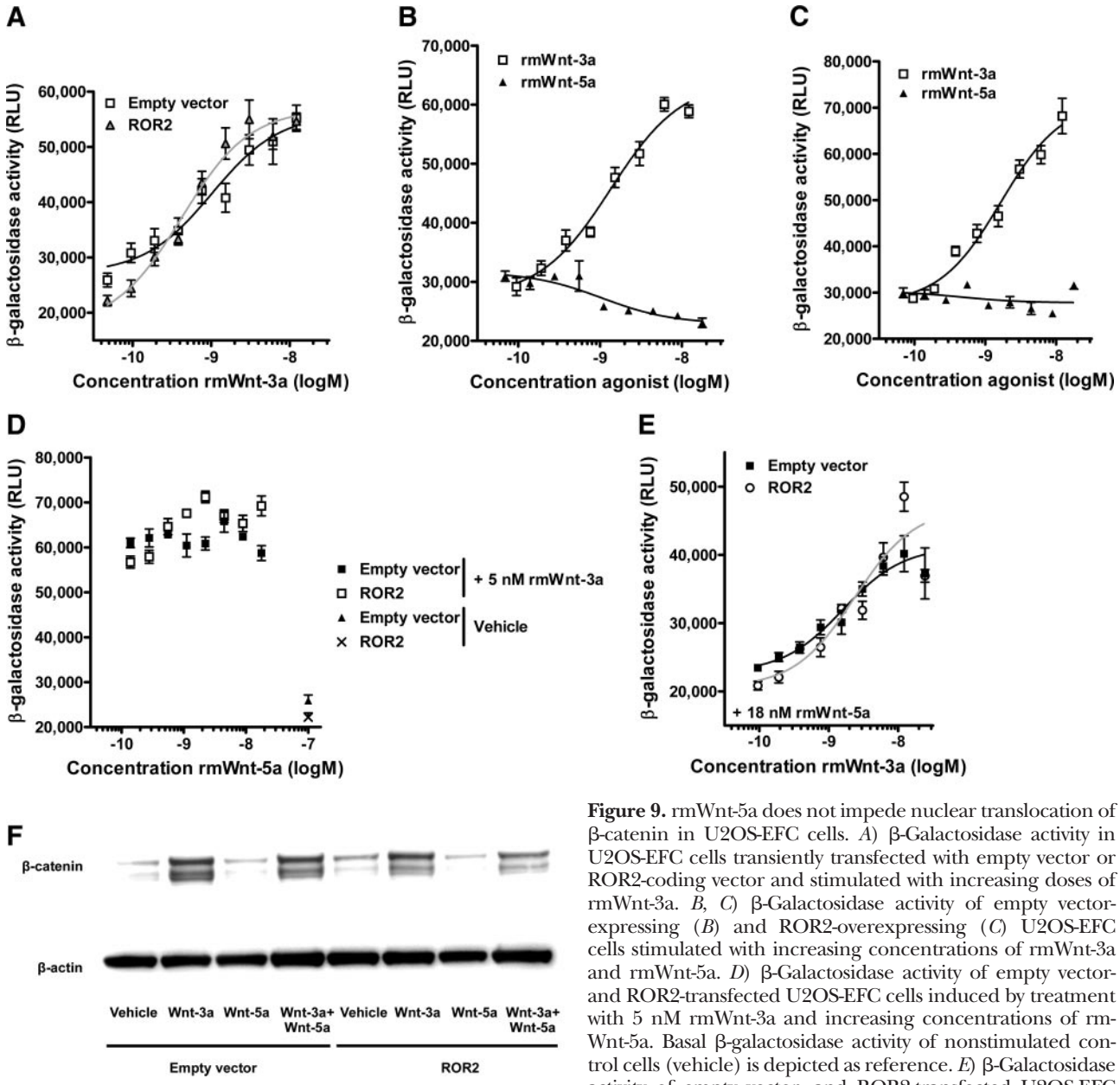

Figure 9. rmWnt-5a does not impede nuclear translocation of β-catenin in U2OS-EFC cells. *A*) β-Galactosidase activity in U2OS-EFC cells transiently transfected with empty vector or ROR2-coding vector and stimulated with increasing doses of rmWnt-3a. *B, C*) β-Galactosidase activity of empty vector-expressing (*B*) and ROR2-overexpressing (*C*) U2OS-EFC cells stimulated with increasing concentrations of rmWnt-3a and rmWnt-5a. *D*) β-Galactosidase activity of empty vector- and ROR2-transfected U2OS-EFC cells induced by treatment with 5 nM rmWnt-3a and increasing concentrations of rmWnt-5a. Basal β-galactosidase activity of nonstimulated control cells (vehicle) is depicted as reference. *E*) β-Galactosidase activity of empty vector- and ROR2-transfected U2OS-EFC cells stimulated with increasing doses of rmWnt-3a in the presence of 18 nM rmWnt-5a. *F*) Western blot analysis of cytoplasmic β-catenin levels in empty vector- and ROR2-transfected U2OS-EFC cells stimulated with 5 nM rmWnt-3a and/or 18 nM rmWnt-5a, or treated with vehicle.

ticals (Basel, Switzerland). We found that sotrastaurin induced SuperTOPflash reporter gene activity in HEK293T cells (Fig. 11*B*). In contrast, we found that PKC reference inhibitors from other chemical series, such as the 5′-nitropyridine compound 1 (36) or 4-aryl pyrimidine compound 2 (37) (**Table 1**), did not activate β-catenin signaling (Fig. 11*A, B*). U2OS-EFC and HEK293T cells treated with 10 μM sotrastaurin displayed significantly elevated levels of cytoplasmic β-catenin, as assessed by Western blot analysis (Fig. 11*C*). We also studied the stabilization of β-catenin in a high-content assay measuring the accumulation and trafficking of β-catenin tagged with green fluorescent protein (GFP). U2OS cells stably expressing β-catenin-GFP fusion protein (U2OS-β-catenin-GFP cells) were treated with sotrastaurin and monitored for β-catenin-GFP accumulation and nuclear translocation by fluorescence microscopy. In vehicle-treated cells, low levels of β-catenin-GFP were found in close association with the plasma membrane (data not shown). For the images shown in Fig. 11*D,* we chose to adjust the settings of the fluorescence microscope to hide this background, however. Strikingly, stimulation of U2OS-β-catenin-GFP cells with rmWnt-3a at concentrations up to 25 nM did not result in any noticeable changes in β-catenin-GFP protein levels or localization (data not shown). Apparently, the assay lacks the sensitivity necessary to measure the subtle differences in β-catenin abundance elicited by natural Wnt ligand. However, treatment of the cells with 10 μM sotrastaurin resulted in an increased abundance and nuclear localization of β-catenin-GFP in ~50% of the cells (Fig. 11*D*). A similar effect was seen on treatment with 30 mM LiCl (Fig. 11*D*). These

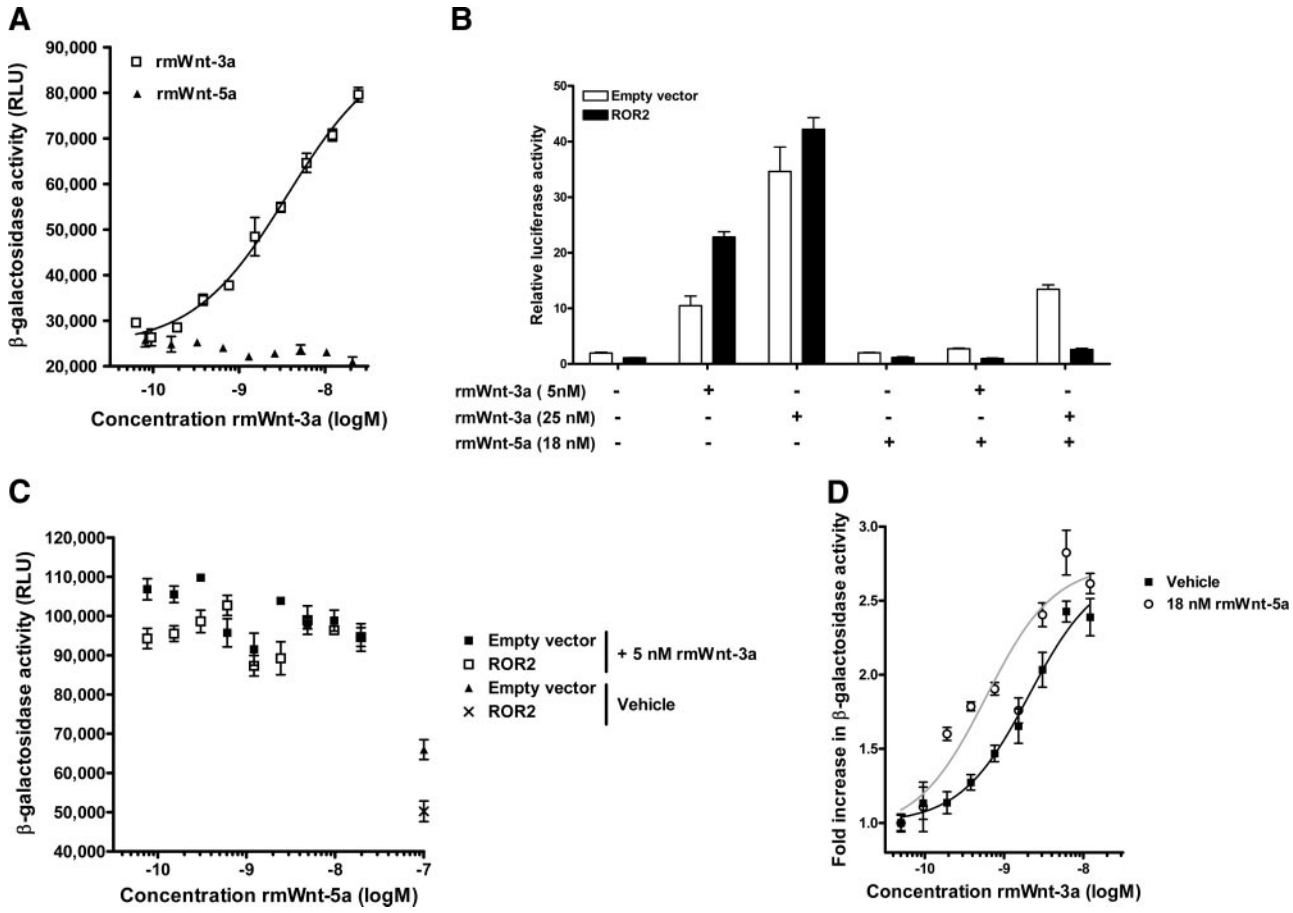

Figure 10. rmWnt-5a does not inhibit nuclear translocation of β-catenin in HEK293-EFC cells. *A*) β-Galactosidase activity of HEK293-EFC cells treated with increasing doses of rmWnt-3a and rmWnt-5a for 3 h. *B*) Luciferase reporter gene activity of HEK293-EFC cells transiently transfected with SuperTOPflash and either ROR2-coding vector or corresponding empty vector, followed by treatment with increasing doses of rmWnt-3a (5 nM and 25 nM, respectively) in the absence or presence of 18 nM rmWnt-5a. *C*) β-Galactosidase activity of empty vector- and ROR2-transfected HEK293-EFC cells induced by treatment with 5 nM rmWnt-3a and increasing concentrations of rmWnt-5a. Basal β-galactosidase activity of nonstimulated control cells (vehicle) is depicted as reference. *D*) Fold increase in β-galactosidase activity of HEK293-EFC cells transiently transfected with ROR2-coding vector and treated with increasing concentrations of rmWnt-3a in the presence or absence of 18 nM rmWnt-5a.

data confirm that sotrastaurin can induce redistribution of β-catenin from the cytoplasm to the nucleus.

Sotrastaurin is a potent immunosuppressant and has been shown to be efficacious in psoriasis patients (33) and various models of experimental transplantation (34). The immunosuppressive activity of sotrastaurin has been attributed to its (sub)nanomolar potency of inhibition of various PKC isoforms, in particular PKCα and PKCθ (33). We confirmed these activities in biochemical assays using immobilized metal ion-affinity based fluorescence polarization (IMAP) (Table 1) (35). We also determined the inhibitory cellular activity of sotrastaurin on activation of antigen-stimulated T cell receptor by measuring the secretion of interleukin 2 (IL-2) from Jurkat T cells or primary blood mononuclear cells (PBMCs), after challenging with anti-CD3 antibody or staphylococcal enterotoxin B, respectively. Sotrastaurin showed nanomolar activity in both assays (Table 1). In view of this high cellular potency, we considered it unlikely that the activation of β-catenin signaling at micromolar concentrations was due to inhibition of PKC. In addition, PKC inhibitor compounds 1 and 2 did not activate Wnt/β-catenin signaling (Fig. 11*A, B*), whereas they potently inhibited PKC (Table 1). We therefore reasoned that sotrastaurin's activity in the EFC assay was probably due to the inhibition of other protein kinases. To identify possible candidate targets, we profiled 100 nM sotrastaurin over a panel of 218 kinases using ^{32}P incorporation assays (performed at Millipore, Dundee, UK). At this concentration, sotrastaurin fully inhibited several PKC isoforms, whereas the activity of most kinases was unaffected (**Fig. 12*A***). Of note, the kinase activity of both isoforms of GSK3 was inhibited by >85% (Supplemental Table S1). Dose-response relations revealed IC_{50}s of 229 nM and 172 nM for GSK3α and GSK3β, respectively (Fig. 12*B* and Table 1). Compound 1 or 2 did not inhibit GSK3 (Table 1). Also, the two other hits from the screen did not inhibit GSK3 (IC_{50}>10 μM), and their mechanism of action is under investigation. The higher potency of sotrastaurin in the biochemical GSK3 assays in comparison to the β-catenin EFC assay can be explained by differences in the concentrations of ATP in the two assays: 50 μM in the biochemical assay *vs.* 1–5 mM in cells (38). Shifts in potencies were also seen between biochemical and cellular assays for PKCs (Table 1) and are commonly observed

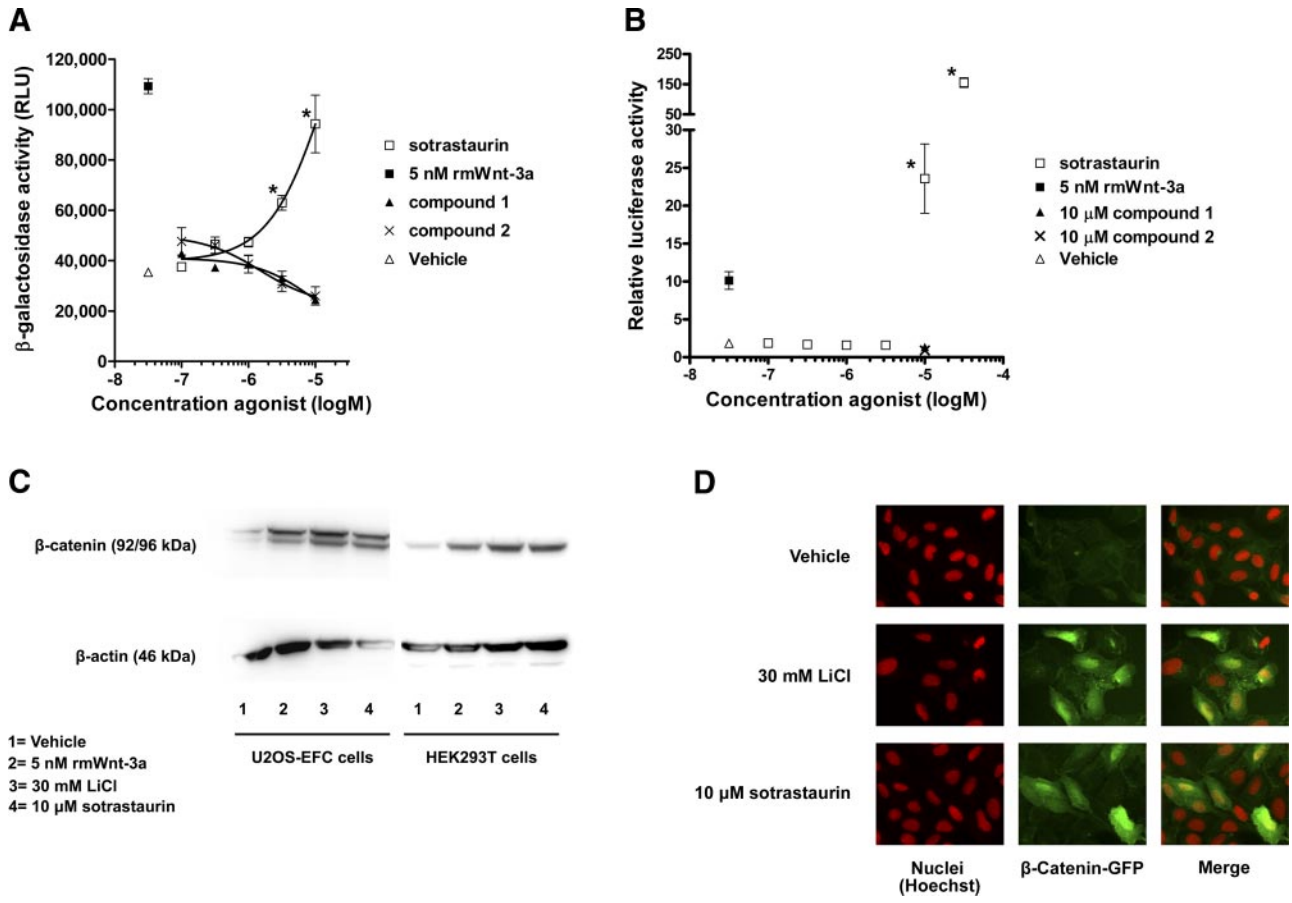

Figure 11. Protein kinase C (PKC) inhibitor sotrastaurin activates Wnt/β-catenin signaling. *A*) U2OS-EFC cells were treated with increasing concentrations of PKC inhibitor (sotrastaurin and the structurally unrelated PKC inhibitor compounds 1 and 2) for 3 h before measurement of β-galactosidase activity. *B*) HEK293T cells transiently transfected with SuperTOPflash reporter gene construct were treated with vehicle, 10 μM PKC inhibitor compound 1 and 2, 5 nM rmWnt-3a, or increasing concentrations of sotrastaurin overnight before luciferase activities were determined. *C*) U2OS-EFC and HEK293T cells were treated with vehicle, 5 nM rmWnt-3a, 30 mM LiCl, or 10 μM sotrastaurin for 3 h. Cytoplasmic extracts of these cells were probed for β-catenin and β-actin by Western blotting. *D*) U2OS cells stably overexpressing a β-catenin-GFP fusion protein were challenged with vehicle, 30 mM LiCl, or 10 μM sotrastaurin overnight and then washed, fixed, and stained with 1 μM Hoechst. Cells were inspected with fluorescence microscopy. $*P < 0.05$ vs. vehicle control; Student's *t* test.

for ATP-competitive kinase inhibitors (38). Altogether, these data indicate that sotrastaurin activates Wnt/β-catenin signaling through inhibition of GSK3.

DISCUSSION

β-Galactosidase EFC is both a specific and a sensitive tool for pathway analysis and drug discovery (18). In this study, we have implemented β-galactosidase EFC to quantify nuclear translocation of β-catenin. We showed that β-galactosidase activity in the U2OS-EFC cell line reflects Wnt/β-catenin activation, based on our observations that β-galactosidase activity correlated with hallmarks of Wnt/β-catenin signaling, such as cytoplasmic stabilization of β-catenin protein and activation of SuperTOPflash reporter gene expression; by using specific blockers, we showed that β-catenin EFC was

TABLE 1. *Inhibitory potency of sotrastaurin, compound 1, and compound 2 in enzymatic and cell-based kinase assays*

	Biochemical				Cellular	
Compound	PKCα	PKCθ	GSK3α	GSK3β	Jurkat IL-2	PBMC IL-2
Sotrastaurin	1.05 ± 0.16 (8)	0.20 ± 0.04 (9)	229	172	6.71 ± 3.76 (10)	4.84 ± 1.70 (7)
Compound 1	>2000 (3)	0.82 ± 0.17 (4)	>10,000	>10,000	22.35 ± 8.67 (5)	13.58 ± 5.88 (4)
Compound 2	20.98 ± 5.82 (8)	6.12 ± 1.03 (8)	>10,000	>10,000	151.19 ± 45.69 (8)	334.41 ± 27.17 (3)

Enzyme activity of PKCα and PKCθ was measured with immobilized metal ion-affinity based fluorescence polarization (IMAP); GSK3α and GSKβ using radiometric assay. IL-2 secretion by Jurkat T cells and PBMCs was measured with ELISA. Values for PKC and cellular assays are mean ± SD IC_{50} (nM), with the number of independent experiments indicated in parentheses. Each experiment consisted of duplicate 10-point dose-response curve determinations. Values for GSK3 assays are IC_{50} based on duplicate 10-point dose-response curves.

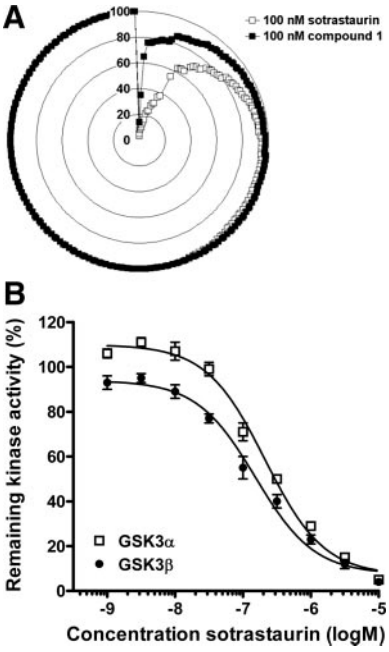

Figure 12. Inhibition of glycogen synthase kinase 3 (GSK3) activity is a likely mechanism of action for sotrastaurin's ability to induce Wnt/β-catenin signaling. *A*) Kinase selectivity profile of sotrastaurin and compound 1. Circle graphs show remaining activity (%) of 218 different kinases examined in ^{32}P incorporation assays in the presence of 100 nM sotrastaurin or compound 1; each dot represents one kinase. *B*) Ability of GSK3α and GSK3β to phosphorylate substrate peptides was analyzed using ^{32}P incorporation assays in the presence of increasing concentrations of sotrastaurin.

dependent on new translation and not transcription; kinetics of rmWnt-3a-stimulated β-galactosidase activity correlated with nuclear accumulation of β-catenin as reported by others (27); and finally, we showed that targeted knockdown of β-catenin with siRNA impaired basal and Wnt-induced β-galactosidase activity, proving specificity of the assay signal.

We exemplified the applicability of β-catenin EFC as a tool for basic research by studying the mechanism of Wnt-5a-mediated inhibition of Wnt/β-catenin signaling (30, 31). Our data indicate that both pathways converge in the nucleus, in agreement with Mikels and Nusse (5). We also showed that the U2OS-EFC cell line can be used to screen small-molecule compound libraries to identify activators of β-catenin signaling. The screen was highly accurate, as we found no false-positive hits.

The immunosuppressant sotrastaurin was identified as an activator of β-catenin nuclear entry. It was confirmed that the compound stabilizes endogenous β-catenin and can induce TCF-dependent transcription at micromolar concentrations. Kinome profiling revealed that sotrastaurin cross-reacts with both isoforms of GSK3, providing a plausible explanation for its ability to induce β-catenin signaling. Although activation of Wnt/β-catenin signaling is associated with many tumor types (6, 7), it is debated whether GSK3-inhibition leads to oncogenic transformation. Of note, lithium therapy in humans with bipolar disorder has not resulted in an increased incidence of colon cancers in these patients (39). Also, mice carrying a germline loss-of-function mutation in APC (APC^{min} mice) did not develop more colon cancers after a diet of lithium (40). In fact, GSK3 inhibitors may have therapeutical potential for the treatment of Alzheimer's disease, diabetes, osteoporosis, and psychiatric disorders (9). The β-catenin EFC assay can be employed to identify starting points for the development of such compounds.

In conclusion, we have devised a fast, easy, reliable, and cost-effective cellular assay to measure Wnt/β-catenin signaling. Its introduction into the drug discovery process and in basic research will aid in probing this clinically relevant signaling cascade. FJ

The authors thank Els van Doornmalen for assistance with high-content image analysis, and Martine Prinsen, Duby Ballak, Lonneke Voorneveld, and Bridget Bulwer for technical assistance. The authors thank Ruben Smeets, Martin Smit, and Jac Wijkmans for critical reading of the manuscript. Prof. Dr. Randall Moon (University of Washington, Seattle, WA, USA), Prof. Dr. Yasuhiro Minami (Kobe University, Kobe, Japan), and Dr. Jan Kitajewski (Columbia University, New York, NY, USA) are acknowledged for providing plasmids. This research is supported by The Netherlands BSIK program (to F.V., W.M.B., and J.F.M.S.).

REFERENCES

1. Logan, C. Y., and Nusse, R. (2004) The Wnt signaling pathway in development and disease. *Annu. Rev. Cell Dev. Biol.* **20,** 781–810
2. Molenaar, M., van de Wetering, W. M., Oosterwegel, M., Peterson-Maduro, J., Godsave, S., Korinek, V., Roose, J., Destree, O., and Clevers, H. (1996) XTcf-3 transcription factor mediates beta-catenin-induced axis formation in *Xenopus* embryos. *Cell* **86,** 391–399
3. Shimizu, H., Julius, M. A., Giarre, M., Zheng, Z., Brown, A. M., and Kitajewski, J. (1997) Transformation by Wnt family proteins correlates with regulation of beta-catenin. *Cell Growth Differ.* **8,** 1349–1358
4. Du, S. J., Purcell, S. M., Christian, J. L., McGrew, L. L., and Moon, R. T. (1995) Identification of distinct classes and functional domains of Wnts through expression of wild-type and chimeric proteins in *Xenopus* embryos. *Mol. Cell. Biol.* **15,** 2625–2634
5. Mikels, A. J., and Nusse, R. (2006) Purified Wnt5a protein activates or inhibits β-catenin-TCF signaling depending on receptor context. *PLoS Biol.* **4,** e115
6. Barker, N., and Clevers, H. (2006) Mining the Wnt pathway for cancer therapeutics. *Nat. Rev. Drug Discov.* **5,** 997–1014
7. Clevers, H. (2006) Wnt/beta-catenin signaling in development and disease. *Cell* **127,** 469–480
8. Baron, R., Rawadi, G., and Roman-Roman, S. (2006) Wnt signaling: a key regulator of bone mass. *Curr. Top. Dev. Biol.* **76,** 103–127
9. Jope, R. S., Yuskaitis, C. J., and Beurel, E. (2007) Glycogen synthase kinase-3 (GSK3): inflammation, diseases, and therapeutics. *Neurochem. Res.* **32,** 577–595
10. Morrell, N. T., Leucht, P., Zhao, L., Kim, J. B., ten Berge, D., Ponnusamy, K., Carre, A. L., Dudek, H., Zachlederova, M., McElhaney, M., Brunton, S., Gunzner, J., Callow, M., Polakis, P., Costa, M., Zhang, X. M., Helms, J. A., and Nusse, R. (2008) Liposomal packaging generates Wnt protein with in vivo biological activity. *PLoS ONE* **3,** e2930
11. Chen, B., Dodge, M. E., Tang, W., Lu, J., Ma, Z., Fan, C. W., Wei, S., Hao, W., Kilgore, J., Williams, N. S., Roth, M. G., Amatruda, J. F., Chen, C., and Lum, L. (2009) Small molecule-mediated disruption of Wnt-dependent signaling in tissue regeneration and Cancer. *Nat. Chem. Biol.* **5,** 100–107
12. Crisman, T. J., Parker, C. N., Jenkins, J. L., Scheiber, J., Thoma, M., Kang, Z. B., Kim, R., Bender, A., Nettles, J. H., Davies, J. W.,

and Glick, M. (2007) Understanding false positives in reporter gene assays: in silico chemogenomics approaches to prioritize cell-based HTS data. *J. Chem. Inf. Model.* **47,** 1319–1327
13. Borchert, K. M., Galvin, R. J., Frolik, C. A., Hale, L. V., Halladay, D. L., Gonyier, R. J., Trask, O. J., Nickischer, D. R., and Houck, K. A. (2005) High-content screening assay for activators of the Wnt/Fzd pathway in primary human cells. *Assay Drug Dev. Technol.* **3,** 133–141
14. Borchert, K. M., Sells Galvin, R. J., Hale, L. V., Trask, O. J., Nickischer, D. R., and Houck, K. A. (2006) Screening for activators of the wingless type/Frizzled pathway by automated fluorescent microscopy. *Methods Enzymol.* **414,** 140–150
15. Zhu, P. J., Zheng, W., Auld, D. S., Jadhav, A., Macarthur, R., Olson, K. R., Peng, K., Dotimas, H., Austin, C. P., and Inglese, J. (2008) A miniaturized glucocorticoid receptor translocation assay using enzymatic fragment complementation evaluated with qHTS. *Comb. Chem. High Throughput Screen.* **11,** 545–559
16. Van der Lee, M. M., Bras, M., van Koppen, C. J., and Zaman, G. J. R. (2008) β-Arrestin recruitment assay for the identification of agonists of the sphingosine 1-phosphate receptor EDG1. *J. Biomol. Screen.* **13,** 986–998
17. Jacob, F., and Monod, J. (1961) Genetic regulatory mechanisms in the synthesis of proteins. *J. Mol. Biol.* **3,** 318–356
18. Wehrman, T. S., Casipit, C. L., Gewertz, N. M., and Blau, H. M. (2005) Enzymatic detection of protein translocation. *Nat. Methods* **2,** 521–527
19. Horecka, J., Charter, N. W., Bosano, B. L., Fung, P., Kobel, P., Peng, K., and Eglen, R. M. (2006) Antibody-free method for protein detection on blots using enzyme fragment complementation. *BioTechniques* **40,** 381–383
20. Binnerts, M. E., Kim, K. A., Bright, J. M., Patel, S. M., Tran, K., Zhou, M., Leung, J. M., Liu, Y., Lomas, W. E., III, Dixon, M., Hazell, S. A., Wagle, M., Nie, W. S., Tomasevic, N., Williams, J., Zhan, X., Levy, M. D., Funk, W. D., and Abo, A. (2007) R-Spondin1 regulates Wnt signaling by inhibiting internalization of LRP6. *Proc. Natl. Acad. Sci. U. S. A.* **104,** 14700–14705
21. Verkaar, F., van Rosmalen, J. W., Smits, J. F., Blankesteijn, W. M., and Zaman, G. J. R. (2009) Stably overexpressed human Frizzled-2 signals through the beta-catenin pathway and does not activate Ca^{2+}-mobilization in human embryonic kidney 293 cells. *Cell. Signal.* **21,** 22–33
22. Klein, P. S., and Melton, D. A. (1996) A molecular mechanism for the effect of lithium on development. *Proc. Natl. Acad. Sci. U. S. A.* **93,** 8455–8459
23. Rock, K. L., Gramm, C., Rothstein, L., Clark, K., Stein, R., Dick, L., Hwang, D., and Goldberg, A. L. (1994) Inhibitors of the proteasome block the degradation of most cell proteins and the generation of peptides presented on MHC class I molecules. *Cell* **78,** 761–771
24. Polakis, P. (2007) The many ways of Wnt in cancer. *Curr. Opin. Genet. Dev.* **17,** 45–51
25. Veeman, M. T., Slusarski, D. C., Kaykas, A., Louie, S. H., and Moon, R. T. (2003) Zebrafish prickle, a modulator of noncanonical Wnt/Fz signaling, regulates gastrulation movements. *Curr. Biol.* **13,** 680–685
26. Naik, S., and Piwnica-Worms, D. (2007) Real-time imaging of beta-catenin dynamics in cells and living mice. *Proc. Natl. Acad. Sci. U. S. A.* **104,** 17465–17470
27. Yokoyama, N., Yin, D., and Malbon, C. C. (2007) Abundance, complexation, and trafficking of Wnt/beta-catenin signaling elements in response to Wnt3a. *J. Mol. Signal.* **2,** 11
28. Hannoush, R. N. (2008) Kinetics of Wnt-driven β-catenin stabilization revealed by quantitative and temporal imaging. *PLoS ONE* **3,** e3498
29. Tamai, K., Zeng, X., Liu, C., Zhang, X., Harada, Y., Chang, Z., and He, X. (2004) A mechanism for Wnt coreceptor activation. *Mol. Cell* **13,** 149–156
30. Torres, M. A., Yang-Snyder, J. A., Purcell, S. M., DeMarais, A. A., McGrew, L. L., and Moon, R. T. (1996) Activities of the Wnt-1 class of secreted signaling factors are antagonized by the Wnt-5A class and by a dominant negative cadherin in early *Xenopus* development. *J. Cell Biol.* **133,** 1123–1137
31. Topol, L., Jiang, X., Choi, H., Garrett-Beal, L., Carolan, P. J., and Yang, Y. (2003) Wnt-5a inhibits the canonical Wnt pathway by promoting GSK-3-independent beta-catenin degradation. *J. Cell Biol.* **162,** 899–908
32. Zhang, J. H., Chung, T. D., and Oldenburg, K. R. (1999) A simple statistical parameter for use in evaluation and validation of high throughput screening assays. *J. Biomol. Screen.* **4,** 67–73
33. Skvara, H., Dawid, M., Kleyn, E., Wolff, B., Meingassner, J. G., Knight, H., Dumortier, T., Kopp, T., Fallahi, N., Stary, G., Burkhart, C., Grenet, O., Wagner, J., Hijazi, Y., Morris, R. E., McGeown, C., Rordorf, C., Griffiths, C. E., Stingl, G., and Jung, T. (2008) The PKC inhibitor AEB071 may be a therapeutic option for psoriasis. *J. Clin. Invest.* **118,** 3151–3159
34. Merani, S., Pawlick, R. L., Edgar, R. L., Toso, C., Emamaullee, J., Anderson, C. C., and Shapiro, A. M. (2009) Protein kinase C inhibitor, *AEB-071*, acts complementarily with cyclosporine to prevent islet rejection in rats. *Transplantation* **87,** 59–65
35. Loomans, E. E., van Doornmalen, A. M., Wat, J. W., and Zaman, G. J. (2003) High-throughput screening with immobilized metal ion affinity-based fluorescence polarization detection, a homogeneous assay for protein kinases. *Assay Drug Dev. Technol.* **1,** 445–453
36. Cywin, C. L., Dahmann, G., Prokopowicz, A. S III., Young, E. R., Magolda, R. L., Cardozo, M. G., Cogan, D. A., Disalvo, D., Ginn, J. D., Kashem, M. A., Wolak, J. P., Homon, C. A., Farrell, T. M., Grbic, H., Hu, H., Kaplita, P. V., Liu, L. H., Spero, D. M., Jeanfavre, D. D., O'Shea, K. M., White, D. M., Woska, J. R., Jr., and Brown, M. L. (2007) Discovery of potent and selective PKC-theta inhibitors. *Bioorg. Med. Chem. Lett.* **17,** 225–230
37. Fleming, P. E., Shi, Z., Chen, S., Schmidt, J. F., Reader, J. C., Hone, N. D., and Ciavarri, J. P. (2009) 2-(amino-substituted)-4-aryl pyramidines and related compounds useful for treating inflammatory diseases. Patent no. WO 2005/066139 A2
38. Knight, Z. A., and Shokat, K. M. (2005) Features of selective kinase inhibitors. *Chem. Biol.* **12,** 621–637
39. Cohen, Y., Chetrit, A., Cohen, Y., Sirota, P., and Modan, B. (1998) Cancer morbidity in psychiatric patients: influence of lithium carbonate treatment. *Med. Oncol.* **15,** 32–36
40. Gould, T. D., Gray, N. A., and Manji, H. K. (2003) Effects of a glycogen synthase kinase-3 inhibitor, lithium, in adenomatous polyposis coli mutant mice. *Pharmacol. Res.* **48,** 49–53

Received for publication July 20, 2009.
Accepted for publication November 5, 2009.